

SIZE-SELECTIVE CONCENTRATION OF CHONDRULES AND OTHER SMALL PARTICLES IN PROTOPLANETARY NEBULA TURBULENCE

JEFFREY N. CUZZI,¹ ROBERT C. HOGAN,² JULIE M. PAQUE,³ AND ANTHONY R. DOBROVOLSIS⁴

Mail Stop 245-3, Moffett Field, CA 94035-1000.

Received 2000 February 23; accepted 2000 August 14

ABSTRACT

Size-selective concentration of particles in a weakly turbulent protoplanetary nebula may be responsible for the initial collection of chondrules and other constituents into primitive body precursors. This paper presents the main elements of this process of *turbulent concentration*. In the terrestrial planet region, both the characteristic size and size distribution of chondrules are explained. “Fluffier” particles would be concentrated in nebula regions that were at a lower gas density and/or more intensely turbulent. The spatial distribution of concentrated particle density obeys multifractal scaling, suggesting a close tie to the turbulent cascade process. This scaling behavior allows predictions of the probability distributions for concentration in the protoplanetary nebula to be made. Large concentration factors ($>10^5$) are readily obtained, implying that numerous zones of particle density significantly exceeding the gas density could exist. If most of the available solids were actually in chondrule-sized particles, the ensuing particle mass density would become so large that the feedback effects on gas turbulence due to mass loading could no longer be neglected. This paper describes the process, presenting its basic elements and some implications, without including the effects of mass loading.

Subject headings: planetary systems — solar system: formation — stars: formation

1. BACKGROUND AND INTRODUCTION

Primitive (unmelted) chondritic meteorites are composed in large part of millimeter-sized, once-molten silicate particles (chondrules) and metallic grains out of mineralogical equilibrium with each other. Many chondrites contain inclusions of refractory minerals that have been dated as the oldest objects formed in the solar system (MacPherson et al. 1989, 1995). The chemical, isotopic, mineralogical, and petrographic properties of individual chondrules themselves imply that independent entities were melted by some “flash heating” event in the gaseous protoplanetary nebula, and remained molten for fairly short times (less than 1 hr; Jones et al. 2000). Chondrules are diverse in chemistry but are narrowly size-sorted (Grossman et al. 1989; Brearley & Jones 1999), apparently by their aerodynamic cross section (Dodd 1976; Skinner & Leenhouts 1991; Keubler et al. 1999); the least mechanically evolved pieces in chondrites have the appearance of being gently brought together (Metzler et al. 1992) and subsequently compacted to solid density. Various hypotheses have been advanced to explain these properties (see, e.g., Boss 1996, Hewins, Jones, & Scott 1996, Hewins 1997, Connolly & Love 1998, and Jones et al. 2000 for recent general reviews and discussion), but the puzzle remains unsolved. The fact that many primitive meteorites are composed of up to 70%–80% chondrules by volume (Grossman et al. 1989) implies that the chondrule formation and accumulation processes were of widespread and significant importance in the very earliest stages of the accretion of the asteroidal objects which provide the parent bodies for these primitive meteorites. Since the terrestrial planets apparently formed from various proportions of

known meteorite types, one expects that the process extended beyond the current asteroid belt and that understanding these early stages is important for understanding planetary accretion overall. These stages of circumstellar disk evolution relate to regions and epochs when the particulate opacity is high, but when some particle growth has occurred—and are thus also of great interest for study at infrared and millimeter wavelengths.

Prior work (Dubrulle, Sterzik, & Morfill 1995; Cuzzi, Dobrovolskis, & Hogan 1996, hereafter CDH96) has pointed out that, unless the turbulent kinetic energy in the nebula gas is vanishingly small (see § 2), chondrule-sized particles are unable to settle individually to the nebula midplane, where most growth to planetesimal size must occur. Instead, CDH96 proposed that, following their initial melting, and throughout multiple recurrences of similar heating events (Wasson 1996; Connolly & Love 1998; Desch & Cuzzi 2000), chondrules pursue an extended free-floating existence under plausible conditions of nebula gas density and turbulent intensity in the terrestrial planet region, successively encountering zones of varying concentration enhancement (§ 5.1), until by chance they encounter an unusually dense zone where they might physically coalesce into much more massive, but still not solid, entities. In a second stage, such entities—dense clusters of particles—might have enough coherence to resist disruption as they settle to the midplane, or to be collected in a different process into the cores of the largest eddies (discussed below) for subsequent accumulation into planetesimals. Or, dense zones may only provide environments of enhanced collisional accumulation of chondrules. The second stage remains unstudied and qualitative; here we focus on the first stage.

The process of interest is known as *preferential concentration* or *turbulent concentration* (TC). The nature of this process is that isotropic, homogeneous, three-dimensional turbulence provides numerous fluid zones of low vorticity

¹ Ames Research Center, NASA; cuzzi@cosmic.arc.nasa.gov.

² Symtech, Inc.; hogan@cosmic.arc.nasa.gov.

³ SETI Institute; jpaque@mail.arc.nasa.gov.

⁴ University of California, Santa Cruz; dobrov@cosmic.arc.nasa.gov.

and high strain in which particles having a narrowly defined range of aerodynamic properties can be significantly, but usually briefly, concentrated (discussed further below). This somewhat counterintuitive effect was first alluded to theoretically (Maxey 1987), subsequently demonstrated numerically (Squires & Eaton 1990, 1991; Wang & Maxey 1993), and recently demonstrated experimentally as well (Fessler, Kulick, & Eaton 1994; for a review see Eaton & Fessler 1994). The concentration factor C is the ratio of the local particle density to its global average. In numerical studies to date (Squires & Eaton 1990, 1991; CDH96; Hogan, Cuzzi, & Dobrovolskis 1999), turbulence with Reynolds numbers of 10^2 – 10^3 contains dense zones where the concentration factors C reach 40–300 for optimally concentrated particles. We extended numerical studies of this effect and applied scaling relationships to predict its behavior under protoplanetary nebula conditions (CDH96; Cuzzi et al. 1998). We found that under canonical inner nebula conditions, particles with the size and density of chondrules would be optimally concentrated. Here we show that the process is easily generalized to a wide range of fluffier particles in lower density regions of the nebula (§ 3).

We note that TC is a quite different process than the superficially similar effect in which far larger (meter-and-larger radius) particles with stopping times comparable to or larger than the eddy times of the largest eddies (with eddy times comparable to the orbit period) can accumulate near the centers of such eddies (Barge & Sommeria 1995; Tanga et al. 1996; Bracco et al. 1999). Klahr & Henning (1997) showed concentration of millimeter-sized particles within large, slow, two-dimensional circulation patterns (not turbulent eddies). However, unless these slow circulation patterns represent the primary kinetic energy reservoir of the (non-Keplerian) fluid motions, concentration of such small particles will not occur. That is, if the nebula turbulence has a normal three-dimensional cascade with its energy peak at spatial and temporal scales that are a small fraction of the nebula scale height and orbital period (as normally implied by turbulent “ α -models” described in § 2), chondrule-sized particles will diffuse faster than they can be concentrated by such large, slow circulation patterns. For example, numerical calculations by Supulver & Lin (2000), which modeled eddy motions on a wide “inertial range” of spatial and temporal scales, as well as our own calculations, show that chondrule-sized particles do not accumulate in large eddies for two reasons: first, their trajectories are mixed by the smaller eddies, and second, “real” eddies in homogeneous turbulence—even the largest ones—dissipate within a single overturn time. Under these circumstances (assumed in this paper), millimeter-sized particles would be nearly uniformly dispersed by three-dimensional turbulence, as one would naively expect for such small particles that are trapped to nearly all fluid parcels, if it were not for the role of turbulent concentration as described herein. The true energy spectrum and dimensionality of nebula turbulence is, however, not currently understood, and is the subject of several active research tasks.

Our emphasis in testing these concepts has been to compare our predictions with the properties of easily identified and studied chondrules and chondrites. For instance, we have now studied the size distribution of preferentially concentrated particles in detail, and found it to be insensitive to, or independent of, Reynolds number (Hogan &

Cuzzi 2000); here we show that this predicted size distribution is in very good agreement with a typical chondrule size distribution (§ 4).

While C does increase systematically with increasing Reynolds number (CDH96), our prior estimates of concentrations at nebula Reynolds numbers, which are plausibly far larger than those accessible to numerical modeling, had required sizeable extrapolations. We have more recently shown that the spatial structure of the concentrated particle density field is a multifractal that has Reynolds-number-independent properties (Hogan et al. 1999) and here will use this result to provide a firmer basis for predictions under nebula conditions. The Reynolds-number independence of key elements of TC is critical, as it frees our predictions from the risk of sizeable extrapolations (§ 5).

The evolution of extremely dense clumps, within which interparticle collisions might entrap particles (CDH96), remains unstudied and will require a better understanding of the behavior of turbulent concentration when the particle mass density exceeds that of the gas and of particle ensembles whose density is large enough to affect the gas flow properties. In § 6 we discuss this important effect.

2. TURBULENCE AND TURBULENT CONCENTRATION (TC)

Homogeneous, isotropic, three-dimensional turbulence is characterized by a cascade of energy through a range of scales, known as the inertial range, from the largest (or integral) spatial scale L , having associated velocity V_L , to the smallest (or Kolmogorov) scale, η , where it is dissipated (Tennekes & Lumley 1972; Hinze 1975). The intensity of the turbulence is characterized by the Reynolds number, which can be written $Re \equiv (L/\eta)^{4/3}$. Since dissipation occurs primarily on the small scales where molecular viscosity comes into play, more energetic (higher Re) flows can drive turbulence through a wider inertial range, to smaller η , for any given viscosity.

Re is ordinarily defined as $Re = LV_L/\nu_m$, where ν_m is the molecular viscosity; Re here is the ratio of transport by macroscopic motions to that by molecular motions. This definition combines the velocity and length scales into a turbulent viscosity ν_T . The Reynolds stresses that appear in angular momentum transport equations are often modeled by this sort of turbulent viscosity (the “ α model” of Shakura & Sunyaev 1973). However, in a Keplerian disk, the mere existence of turbulent motions (turbulent kinetic energy, leading to diffusivity of scalars) does not necessarily imply viscous transport of angular momentum (by a Reynolds stress, or torque, acting as a positive turbulent viscosity; Prinn 1990). This distinction is related to the possibility that the on-diagonal and off-diagonal terms of the stress tensor might have very different relative strengths in Keplerian disks than in more familiar turbulent environments (Kato & Yoshizawa 1997). While astrophysical “ α -models” of protoplanetary disks emphasize turbulent viscosity ν_T in its angular momentum transport role, TC is more closely related to scalar diffusivity, or turbulent kinetic energy per unit mass density k . Therefore, we distinguish two types of the familiar astrophysical α . We first discuss the familiar Shakura-Sunyaev prescription, which defines the turbulent viscosity as $\nu_T = \alpha_v cH$, where c is the sound speed and H is the vertical scale height.

Without external drivers, the overall nebula is likely to be

in a regime of Rossby number $Ro \equiv \Omega_L/\Omega_0$ of order unity, where Ω_L is the largest eddy frequency and Ω_0 is the orbital frequency. We thus rewrite v_T in terms of these fundamental properties:

$$\begin{aligned} v_T &= LV_L = L^2\Omega_L (= V_L^2/\Omega_L) = \alpha_v cH \\ &= \alpha_v H^2\Omega_0 (= \alpha_v c^2/\Omega_0); \end{aligned} \quad (1)$$

thus

$$L = H\sqrt{\alpha_v}\left(\frac{\Omega_0}{\Omega_L}\right)^{1/2}, \quad V_L = c\sqrt{\alpha_v}\left(\frac{\Omega_L}{\Omega_0}\right)^{1/2}. \quad (2)$$

In equation (1) above, the basic expression $v_T = LV_L$ is rewritten to decouple L and V_L , resulting in two separate expressions that both contain the large eddy frequency Ω_L (third and fourth terms) and can separately be equated to their α -model counterparts, which both contain the orbit frequency Ω_0 (sixth and seventh terms, respectively). Primary reliance on frequencies as a way of separating the length and velocity scales is physically justified in a rotating system. We then set equal the third and sixth (fourth and seventh) terms in equation (1), which are the functional equivalents of each other, to get L and V_L separately and in parallel (eq. [2]). With the expectation that Coriolis forces will maintain the frequencies of the largest truly turbulent eddies (those that participate in the turbulent cascade), Ω_L , at values no smaller than, but probably comparable to, the local orbital frequency Ω_0 , we find that $V_L = c\sqrt{\alpha_v}$ and $L = H\sqrt{\alpha_v}$. Occasionally it is assumed that $L \approx H$ (e.g., Morfill 1985), but this implies $V_L = v_T/L = c\alpha_v$ and thus $\Omega_L = V_L/L = c\alpha_v/H = \alpha_v\Omega_0 \ll \Omega_0$, an implausible situation for genuine turbulence. The distinction is important for us, as we need to scale turbulent velocities and length scales independently. The important point is that the scaling parameter α_v is “shared” by the length and velocity scales, rather than being associated with one or the other.

A scaling analysis cannot establish whether fluid motions with arbitrary L and V_L do in fact provide a positive Reynolds stress or “turbulent viscosity” given by their product; conversely, estimates of the magnitude of V_L and L from an observed turbulent viscosity v_T and associated α_v , as above, may misrepresent their actual magnitudes. This is because certain types of spatial correlations between “random” fluid motions are needed to provide a positive Reynolds stress, or turbulent viscosity, and this may not occur in systems that are strongly influenced by rotation or otherwise strongly perturbed (Prinn 1990; Kato & Yoshizawa 1997).

Another approach to determining V_L is based on the turbulent kinetic energy per unit mass k and an associated α_k : $k = \frac{3}{2}V_L^2 \equiv \frac{1}{2}\alpha_k c^2$, or $V_L = c\sqrt{\alpha_k/3}$. The mere presence of turbulent fluid motions with $k \equiv \alpha_k c^2/2 = 3V_L^2/2$ is sufficient to produce turbulent concentration, with no additional uncertainties about the degree and sign of the correlation between orthogonal components of the fluid motions as in α_v (Prinn 1990). While this definition provides no insight into the turbulent length scale L , we presume by analogy to the above argument that $L = H\sqrt{\alpha_k}$. With regard to the nebula, where properties are uncertain, we suppress the factor of $\sqrt{3}$ (effectively ignoring the distinction between a single component of V_L and its magnitude) and approximate the turbulent Reynolds number of the nebula by $Re = \alpha_k cH/v_m$. Angular momentum may still be transported by a turbulent viscosity $v_T = \alpha_v cH$, but

whether $\alpha_v \approx \alpha_k$ or not is peripheral to this work (Kato & Yoshizawa [1997] find that $\alpha_v < \alpha_k$).

Possible sources of k include forcing by ongoing infall onto the disk in the very early stages (Cameron 1978; Prinn 1990), turbulent convection powered by release of gravitational energy into heat as the disk evolves (Lin & Papaloizou 1985; Cabot, Canuto, & Pollack 1987; Goldman & Wandel 1994; Bell et al. 1997), enforced Keplerian differential rotation (Dubrulle 1993), and magnetorotational instability or MRI (Balbus & Hawley 1991, 1998). Typical estimates of α_k from these sources are $\sim 10^{-4}$ to 10^{-1} , and thus $Re = 10^8$ – 10^{11} .

However, uncertainties remain with all of the above mechanisms. The infall stage lasts only a relatively short fraction of the evolution lifetime of typical nebulae, and the magnetorotational instability will not act in the dense inner scale height of the disk where most of the mass and chondrules probably reside (Gammie 1996) and perhaps not even high in the nebula (Desch 2000). The validity of convection and differential rotation, acting by themselves, rests on their uncertain ability to be self-sustaining. This requires turbulence to be able to transport sufficient angular momentum outwards that mass can evolve inwards, releasing gravitational energy to be converted into turbulence. Several studies (most recently Stone & Balbus 1996) found that convective turbulence fails to produce outward angular momentum transport (positive Reynolds stresses). However, some recent three-dimensional numerical studies, which better capture large azimuthal structures, seem to imply that it may in fact be able to do so (Klahr 2000a, 2000b). Of course, as grains accumulate, opacity decreases, and thermal convection may weaken. Differential rotation is free of this limitation (Dubrulle 1993), but numerical and analytical arguments by Balbus, Hawley, & Stone (1996) question differential rotation as a source for turbulence based on the energetics and stability of Keplerian disks. However, Richard, & Zahn (1999) have suggested, based on laboratory analogues, that instability to turbulence in such systems requires a higher Reynolds number than accessible to current numerical models. Kato & Yoshizawa (1997) have shown that Keplerian rotation probably does not preclude some true turbulent viscosity (i.e., positive Reynolds stress, or $\alpha_v > 0$), but as a much smaller fraction of the ambient turbulent kinetic energy (α_k) than under non-Keplerian conditions. Thus, it also remains in doubt whether turbulence driven by differential rotation alone can be self-sustaining. Nonsteady situations might even need to be considered.

In short, the source of angular momentum transport is poorly understood, and it is not clear how disks evolve at all. However, while we still do not understand the mechanism that allows them to do so, protoplanetary disks are observed to evolve with mass accretion rates in the range of $\dot{M} = 10^{-7}$ to $10^{-9} M_\odot \text{ yr}^{-1}$ (Hartmann et al. 1998) and thus have an associated gravitational energy release rate per unit area of $\dot{E}_{\text{grav}} = 3GM_*\dot{M}/4\pi R^3$ (Lüst 1952; Lynden-Bell & Pringle 1974). Here G is the gravitational constant, M_* is the mass of the central star, and R is the distance from the central star.

Turbulent kinetic energy is dissipated at a rate of approximately $\dot{E}_k = 2k\Omega_0\rho_g H = k\Omega_0\Sigma$, where ρ_g is the local gas density and $\Sigma = 2\rho_g H$. If the gravitational energy \dot{E}_{grav} is released where most of the mass resides, and converted into mechanical turbulence with efficiency ξ_T , then for a disk in steady state with \dot{M} independent of radius, $\dot{E}_{\text{grav}}\xi_T = \dot{E}_k$, or

$$\frac{3GM_* \dot{M} \xi_T}{4\pi R^3} = k\Omega_0 \Sigma = \frac{\alpha_k c^2 \Omega_0 \Sigma}{2}. \quad (3)$$

Substituting $\Omega_0^2 = GM_*/R^3$ and $c = H\Omega_0$,

$$\alpha_k = \frac{3\dot{M} \xi_T}{2\pi c H \Sigma}. \quad (4)$$

For a typical “canonical” nebula with $H(R) = 0.05 \text{ AU} (R/1 \text{ AU})^{5/4}$, $c(R) = 1.9 \times 10^5 (R/1 \text{ AU})^{-1/4} \text{ cm s}^{-1}$, and $\Sigma(R) = 1700 \mathcal{F} (R/1 \text{ AU})^{-3/2} \text{ g cm}^{-2}$, with \mathcal{F} being any enhancement in mass over the “minimum mass” nebula density (Hayashi 1981; see also Cuzzi, Dobrovolskis, & Champney 1993), then

$$\alpha_k \approx 1.3 \times 10^{-3} \left(\frac{R}{1 \text{ AU}} \right)^{1/2} \frac{\dot{M}}{10^{-8} M_\odot \text{ yr}^{-1}} \frac{\xi_T}{\mathcal{F}}. \quad (5)$$

Some recent numerical calculations show ξ_T to be at least several percent (H. Klahr 1999, personal communication); thus $\alpha_k \sim 10^{-3}$ to 10^{-4} seems not to be out of the question in the 2–3 AU region where meteorite parent bodies form. Conversely, Dubrulle et al. (1995) have shown that, in order for chondrule-sized particles to settle into a midplane layer having a density approaching that of the gas (a layer of thickness 10^{-2} to $10^{-3}H$), α_k would need to be in the 10^{-8} to 10^{-10} range (see also CDH96). For α_k to be this low, equations (4) and (5) show that the conversion efficiency into turbulence would need to be less than 10^{-5} for a disk with $\dot{M} = 10^{-8} M_\odot \text{ yr}^{-1}$. Thus, in this paper we simply presume the presence of nebula turbulence at a weak level and explore the consequences. Henceforth, we identify the nebula “ α ” as α_k , and treat Re and its associated α as characterized by L and V_L .

We assume the turbulence has a Kolmogorov-type inertial range, within which each length scale l is characterized by velocity $v(l) = V_L(l/L)^{1/3}$ (Tennekes & Lumley 1972; CDH96) and eddy frequency $\omega(l) = v(l)/l = \Omega_0(l/L)^{-2/3}$, where the frequency of the largest eddy $\omega(L) = V_L/L$ is set equal to Ω_0 , the local orbital frequency. Because the most interesting scales for particle concentrations are on the order of $\eta = L\text{Re}^{-3/4} \ll L$, and even $L \approx H\sqrt{\alpha} \ll H$, deviations from isotropy due to rotation are not a major concern. Particles smaller than the gas mean free path (i.e., smaller than several cm radius under nebula conditions) are in the Epstein drag regime (Weidenschilling 1977), and have a stopping time due to gas drag that is

$$t_s = r\rho_s/c\rho_g, \quad (6)$$

where r and ρ_s are particle radius and internal density. The particle Stokes number $\text{St}_l \equiv t_s \omega(l)$ determines the particle response to eddies of a particular size and frequency; previous studies have shown that the optimally concentrated particles have $\text{St}_\eta = t_s \omega(\eta) \approx 1$ (Eaton & Fessler 1994; Hogan & Cuzzi 2000), that is, their stopping time is comparable to the Kolmogorov eddy turnover time.

3. GENERALITY OF TURBULENT CONCENTRATION

Solving the relation $\text{St}_\eta = t_s \omega(\eta) = 1$ under nebula conditions, CDH96 concluded that the optimally concentrated particles in the terrestrial planet region of a minimum mass nebula with $\alpha \sim 10^{-4}$ to 10^{-3} would have radius and density comparable to those of chondrules. Here we generalize TC to the entire range of nebula conditions. Using the

definition for t_s (eq. [6]) to rewrite the expression for $\text{St}_\eta = t_s \omega(\eta) = 1$,

$$\begin{aligned} r\rho_s = c\rho_g t_s = c\rho_g t_\eta &= \frac{c\rho_g}{\Omega_0(\eta/L)^{-2/3}} = \frac{c\rho_g}{\Omega_0 \text{Re}^{1/2}} \\ &= \frac{c\rho_g v_m^{1/2}}{\Omega_0(\alpha c H)^{1/2}}. \end{aligned} \quad (7)$$

CDH96 Substituted $v_m = c\lambda/2 = m_{\text{H}_2} c/2\rho_g \sigma_{\text{H}_2}$, where λ is the molecular mean free path, and $m_{\text{H}_2} = 3.2 \times 10^{-24} \text{ g}$ and $\sigma_{\text{H}_2} = 5.7 \times 10^{-16} \text{ cm}^2$ are the mass and cross section of a hydrogen molecule. However, their expression for λ did not include the finite size or the Maxwellian velocity distribution of the gas molecules (see Kennard 1938, eq. [106d] and [126b]), so their λ was too large by a factor of $4\sqrt{2}$. Rearranging terms from equation (7) and correcting this oversight, we find

$$\begin{aligned} r\rho_s &= \left(\frac{m_{\text{H}_2}}{16\sqrt{2}\sigma_{\text{H}_2}} \right)^{1/2} \left(\frac{\Sigma}{\alpha} \right)^{1/2} \\ &= 6.3 \times 10^{-4} \left(\frac{\mathcal{F}}{\alpha} \right)^{1/2} \left(\frac{R}{1 \text{ AU}} \right)^{-3/4} \text{ g cm}^{-2}, \end{aligned} \quad (8)$$

where $\Sigma(R) = 2\rho_g H$ is surface mass density at some distance in the nebula. In the last term we have adopted a canonical radial dependence of $\Sigma(R) = 1700 \mathcal{F} (R/1 \text{ AU})^{-3/2}$ for a “minimum mass” nebula, with \mathcal{F} being some mass enhancement factor. Protoplanetary nebula mass densities inferred from millimeter continuum observations, while subject to grain opacity uncertainties, are compatible with these assumptions (Beckwith & Sargent 1991).

This relationship is shown in Figure 1 for several different typical locations and two different nebula masses. The range of $r\rho_s$ for most chondrules (Ch), obtained using data in Grossman et al. (1989), is mapped along the line for $R = 2.5 \text{ AU}$, and indicates the range of α required to concentrate them selectively. Higher values of α (more intense turbulence) select smaller and/or lower density particles. In both cases, porous aggregates (PA), having considerably lower radius-density product than chondrules, can be optimally concentrated at the low gas densities that characterize the outer planet region or low density regions high above the nebula midplane. Such porous objects are easily produced because the low relative velocities in turbulence of both porous, low-density aggregates, and their constituent monomers, lead to large sticking efficiency and minimal disruption (Weidenschilling & Cuzzi 1993; Chokshi, Tielens, & Hollenbach 1993; Dominik & Tielens 1997). It has also been suggested that extremely low-density, intensely turbulent regions may concentrate tiny grains or very fluffy aggregates (FA) (Wood 1998). TC may thus have been ubiquitous, helping to initiate the formation of “cometesimals” from porous grain aggregates at 10–30 AU or speeding the accretion of dust particles at high elevations (low gas densities) even in the terrestrial planet region.

However, textural evidence might be difficult to obtain from this regime; subsequent compaction would obliterate evidence for any preferred size or density of easily squashed fluffy constituents. Chondrules and their parent chondrites, by nature of their availability and unique, persistent textures, provide the most obvious initial testing ground for turbulent concentration.

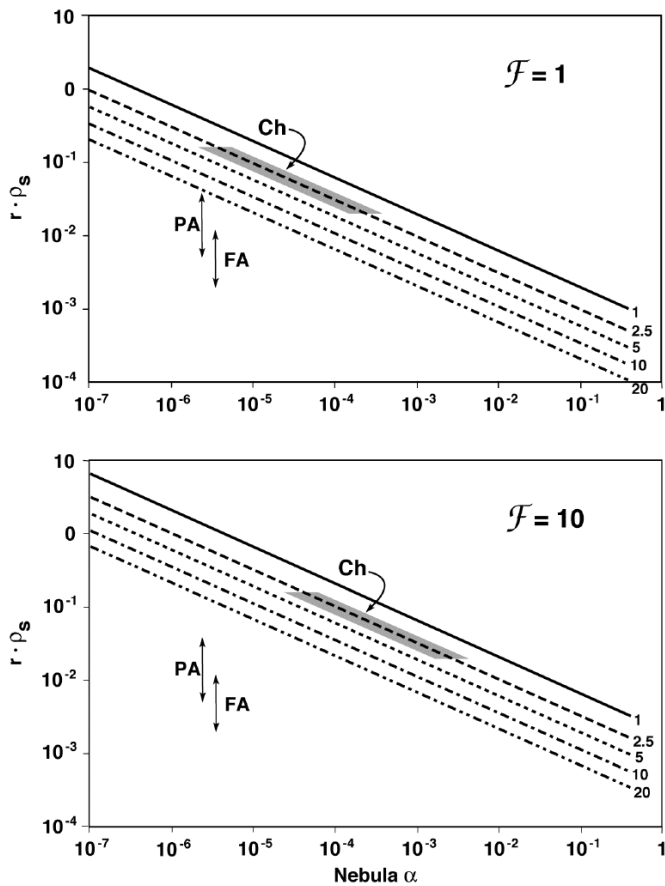


FIG. 1.—Optimal particle radius-density product $r\rho_s$ for turbulent concentration as a function of α at various locations in a typical solar nebula (converted from the optimal Stokes number $St_\eta = 1$ using nominal nebula gas density and local rotation rate). The power-law results are labeled by the appropriate distance from the Sun in AU. (a) Minimum mass nebula ($\mathcal{F} = 1$); solid silicate particles with chondrule sizes and densities (Ch) have the range $r\rho_s \approx 0.015\text{--}0.15$, which would indicate the shaded range of α at 2.5 AU. Smaller gas densities at larger distances from the sun concentrate smaller $r\rho_s$ products (porous aggregates or PA) and even “fluffier” $d = 2$ fractal aggregates (FA) or their monomers, for any α . (b) Somewhat different results obtained assuming an enhanced surface mass density $\mathcal{F} = 10$ times higher than the minimum mass requirement.

4. CONCENTRATED PARTICLE SIZE DISTRIBUTION

If dense clusters of particles are precursors of primitive bodies in any way, the relative abundance as a function of Stokes number St_η for particles in dense regions should show some correspondence to the distributions found in chondrites. To further compare the predictions of TC with meteorite evidence, we have recently determined the detailed form of the size distribution of selectively concentrated particles (Hogan & Cuzzi 2000). Numerical simulations were performed with homogeneous, isotropic, incompressible three-dimensional turbulence at three Reynolds numbers $Re = 62, 246,$ and 765 (these values differ from those given in Hogan et al. 1999 because we now adopt the more correct definition of V_L as one component of the turbulent velocity rather than its magnitude). The particles can be given arbitrary aerodynamic stopping times t_s ; their motions respond only to gas drag and are integrated in the spatial domain. Feedback by the particles onto the gas is not incorporated. The computationally intensive calculations are run on 16 Cray C90 cpus at Ames Research Center. Simulations were initiated with uniform spatial dis-

tributions of particles, themselves uniformly distributed in stopping time over the range $St_\eta = 0.1\text{--}6$, and the relative equilibrium abundance of particles was studied as a function of St_η and C . In the large- C limit of interest, the shape of the relative abundance distribution $\mathcal{A}(St_\eta)$ was found to be independent of both C and Re and only very weakly dependent on the spatial binning assumed (relative to η) (Hogan & Cuzzi 2000). Thus, we believe the numerical results should be valid as a prediction of the size distribution in dense particle concentrations under nebula conditions. The theoretical results are adequately fitted by a lognormal distribution over the core range $St_\eta = 0.5\text{--}2.0$.

We compared our predictions with binned relative abundance data for chondrules disaggregated from one carbonaceous and four ordinary chondrites (Paque & Cuzzi 1997, 2000, in preparation; Cuzzi, Hogan, & Paque 1999). While a few ostensibly similar data sets exist in the literature (e.g., Hughes 1978; Eisenhour 1996; Rubin & Grossman 1987), they generally rely on radii measured microscopically from thin sections of meteorites, or even from disaggregated chondrules, and adopt some average chondrule density $\bar{\rho}_s$. However, recall from equation (6) that the aerodynamic stopping time t_s , which selects particles for TC or any other aerodynamic sorting process, depends on the product $r\rho_s$ for each object. Data for these meteorites imply that merely measuring the chondrule radius distribution and assuming some mean density will slightly, but noticeably, misrepresent the $r\rho_s$ distribution because of chondrule-to-chondrule density variations (Cuzzi et al. 1999).

In Figure 2 we compare the particle abundance shape function $\mathcal{A}(St)$ from our numerical simulations (Hogan & Cuzzi 2000) with the meteorite data. The meteorite histograms were fitted by lognormal functions and aligned horizontally with the predicted histogram by assuming that the optimally concentrated particle size-density product corresponds to $St_\eta = 1$. We conclude that TC by itself can explain the very narrow chondrule size distribution, whatever the chondrule formation process may have produced. There is evidence that both larger and smaller chondrules were created; TC would predict that these nonoptimally sized particles were simply not concentrated to a sufficient degree for eventual incorporation into meteorites unless they were swept up into chondrule rims (if originally smaller) or broken to the proper size (if originally larger). Some particles of arbitrary size will always appear just by accident, perhaps captured by a dense cluster; parent body processes will confuse the situation further.

5. PROBABILITY DISTRIBUTIONS AND MULTIFRACTALS

As mentioned earlier, our numerical results (CDH96) are obtained at Re that are 6 orders of magnitude smaller than plausible nebula Re . Thus, it is very important to understand the Re -scaling of TC properties in detail. We believe this has become possible using a connection between TC and the Re -independent scaling properties of fractals, which are rooted in the properties of the turbulent cascade itself (Hogan et al. 1999; henceforth HCD99). Fractals and multifractals are readily associated with cascade processes. Turbulence (and specifically its inertial range) is the archetype of a cascade process (Tennekes & Lumley 1972; Meneveau & Sreenivasan 1987, 1991), and considerable attention has been devoted to multifractals in turbulence (Frisch & Parisi 1985; Mandelbrot 1989).

A working definition of a fractal is a structure that is

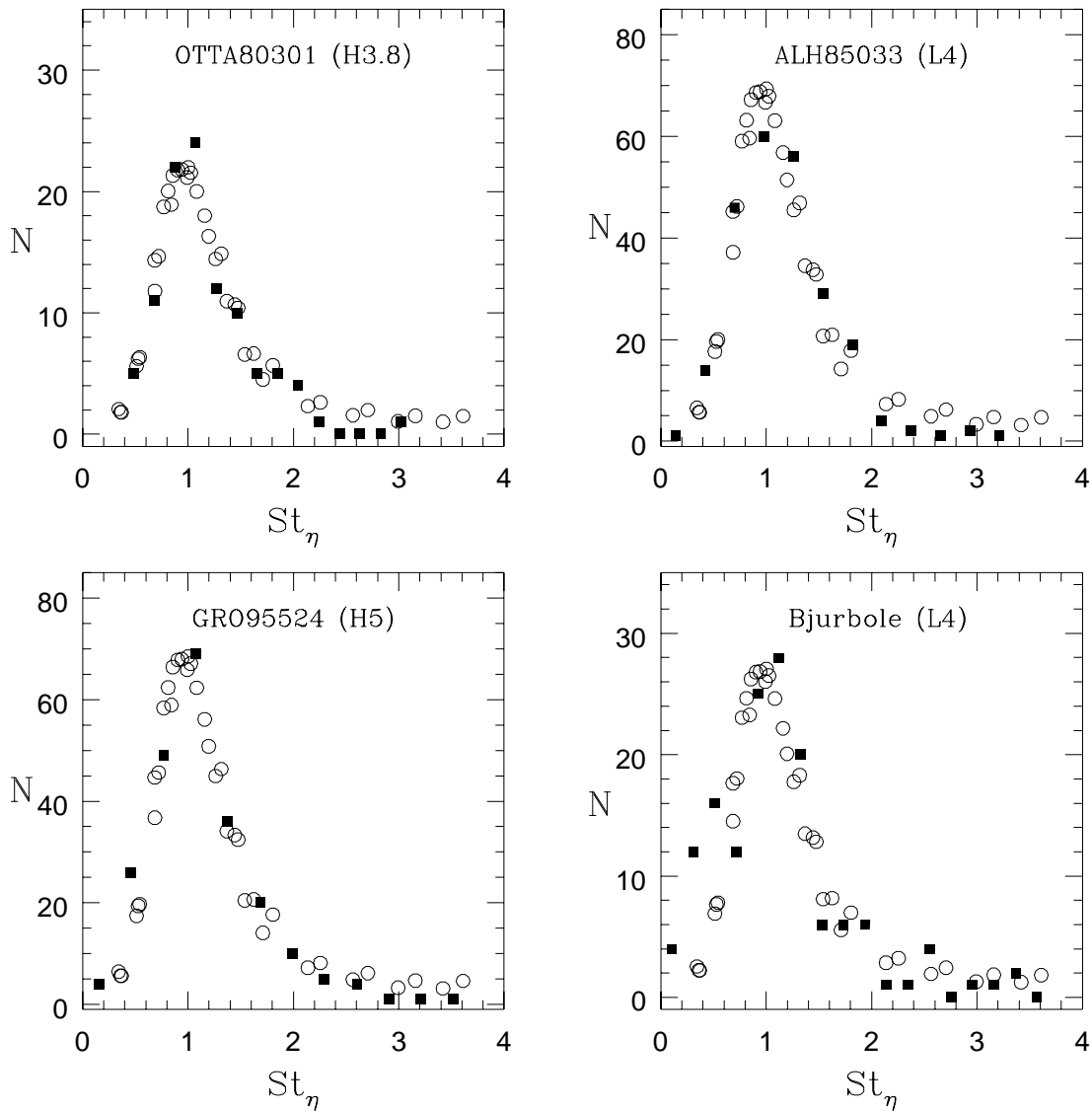


FIG. 2.—Comparison of the size-density distributions of chondrules disaggregated from four ordinary chondrites (*solid symbols*; J. Paque & J. N. Cuzzi 2000, in preparation) with the theoretically determined, Re-independent, shape distribution for the relative abundance of particles concentrated in turbulence as a function of St_η (*open symbols*; Hogan & Cuzzi 2000).

generated by sequential application of a scale-invariant rule on regularly decreasing spatial scales. Simple fractals with constant (but noninteger) dimension are invariant to changes in scale, and result from rules that produce a binary distribution of the local density (say, either 0 or 1). Examples of these are the Cantor set or the Sierpinski gasket (Mandelbrot 1989), in which segments of a line, or portions of a plane, are simply removed without changing the surrounding values. Their average density, as a function of scale ϵ , may be written as $\rho(\epsilon) = \rho_0 \epsilon^{-d}$ with dimension $d = 0.63$ (between a point and a line) and $d = 1.52$ (between a line and a plane), respectively.

In contrast, multifractals result from application of rules (or probability distributions of rules) in which the local measure is changed, while conserving the total measure, by unequal repartitioning of the content of a bin into subbins of regularly decreasing spatial scale. For example, it is easily seen that partitioning some quantity into the two halves of a bin with unequal proportions (say 0.7 and 0.3) raises the mean density in the first half and decreases it in the second.

Repetition of this rule produces some bins that become ever denser with decreasing scale, and others that become ever less dense—with all combinations in between. The ensuing spatial distribution has no well-defined local value in the limit of diminishing bin size; that is, the local values are spatially spiky, “intermittent”, or “singular” (Meneveau & Sreenivasan [1987] present a short and readable discussion of cascade processes and multifractals). The spatial distributions of multifractals are, however, predictable in a statistical sense, using probability distribution functions (PDFs) that are derived directly from their dimensions. For instance, dissipation of turbulent kinetic energy, which occurs on the Kolmogorov spatial scale, is not spatially uniform but has the spatial distribution of a multifractal (Chhabra et al. 1989).

In multifractals, the dimension varies with the value of the measure. In our case, the measure is particle concentration factor C , which is the ratio of the local particle volume density to its global average value. The fractional probability P_i of a particle lying in a bin which contains N_i particles

out of N_p total particles is defined as $P_i = N_i/N_p \equiv \epsilon^{a_i}$, where $\epsilon \equiv$ bin size/domain size. The scaling index a can be viewed as a local dimension for P over some relevant range of scales. The associated concentration factor $C_i \equiv (N_i/v_i)/(N_p/v)$, where v_i is the volume of a bin and v is the total volume of the domain; thus $C_i = (N_i/N_p)/(v_i/v) = (\epsilon^{a_i}/\epsilon^3) = \epsilon^{a_i-3}$. Expressing the bin size, or scale, as some multiple B of η , and the domain size in units of the integral scale as DL , we find the domain normalized bin size to be $\epsilon = B\eta/DL = (B/D)\text{Re}^{-3/4} \equiv 1/\mathcal{R}$, where we have also used the inertial range relationship $\eta = L\text{Re}^{-3/4}$. Thus, $C = \mathcal{R}^{3-a}$, or

$$a = 3 - \frac{\ln C}{\ln \mathcal{R}}. \quad (9)$$

The normalized PDF for a is usually written as a fractional volume $F_v(a) = \rho(a)\epsilon^{3-f(a)}$, where the important function $f(a)$, called the singularity spectrum (Halsey et al. 1986; Chhabra et al. 1989; Mandelbrot 1989), plays the role of a dimension for $F(a)$. The prefactor function $\rho(a)$ is only weakly dependent on scale, and can be approximated as $\sqrt{\ln \mathcal{R}}$ (Chhabra et al. 1989). The function $f(a)$ is discussed more in the next subsection.

We define the PDF $F_v(C)$ as the volume fraction occupied by bins having concentration factor within $(C, C + dC)$, with $\int_{C_{\min}}^{C_{\max}} F_v(C)dC = \int_{a_{\max}}^{a_{\min}} F(a)da \equiv 1$. Transforming variables and their PDFs, we get

$$F_v(C) = F(a) \left| \frac{da}{dC} \right| = \frac{\rho(a)\mathcal{R}^{f(a)-3}}{C \ln \mathcal{R}} \approx \frac{\mathcal{R}^{f(a)-3}}{C\sqrt{\ln \mathcal{R}}}. \quad (10)$$

The fraction of particles occupying bins within $(C, C + dC)$ is defined as $F_p(C) = CF_v(C)$, and both $F_v(C)$ and $F_p(C)$ have cumulative versions $F_v(>C) = \int_C^\infty F_v(C)dC$, and $F_p(>C) = \int_C^\infty F_p(C)dC$. For a stationary, ergodic process, one expects that the fraction of particles having C at any given time [$F_p(C)$] is identical to the fraction of time spent in regions of concentration C by a typical particle, defined as $F_v(C)$. Below, this is confirmed numerically.

5.1. Numerical Results at Low Re

5.1.1. PDFs for Concentration

Using the methodology of Chhabra et al. (1989), we have shown that the spatial distribution of optimally concentrated ($\text{St}_\eta = 1$) particles is a multifractal, and that its singularity spectrum $f(a)$ is invariant over more than an order of magnitude from $\text{Re} = 62$ to $\text{Re} = 765$ (HCD99, who actually give Taylor microscale Reynolds numbers $\text{Re}_\lambda = (15\text{Re})^{1/2} = 40\text{--}140$). This Re -invariance for $f(a)$ is seen only when binning is done on some fundamental flow-relative scale such as a multiple of the Kolmogorov scale η . The function $f(a)$ is found by applying weighted binning techniques to the distribution of interest (Chhabra et al. 1989; HCD99), and depends on both D and B —that is, on the number of integral scales sampled as well as on the binning scale. Careful reassessment of different definitions of the integral scale (see Hinze 1975, chap. 2) has led us to values slightly smaller than those published by HCD99, implying that the computational domain appropriate for our $f(a)$ is $9L$ on a side. Our results for $f(a)$ relative to this domain are shown in Figure 3 (HCD99). The sets with error bars are “quenched,” or averaged over samples each DL in extent. The fact that there is no less than one cell in each sample

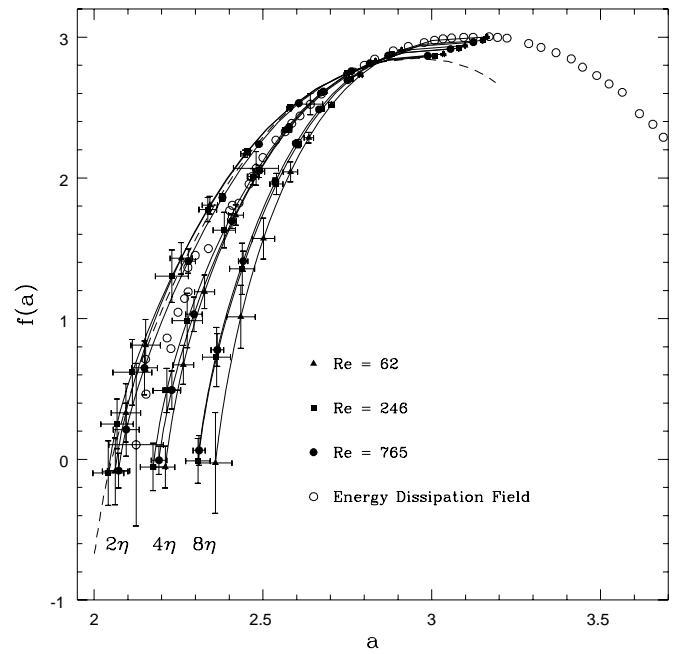


FIG. 3.—Singularity spectra $f(a)$ for particle concentration (solid symbols), for bin sizes of 2, 4, and 8 η , along with error bars representing deviations across many snapshots. The similar looking singularity spectrum for dissipation (open symbols) is from Meneveau & Sreenivasan (1987). Also shown (dashed curve) is our annealed $f(a)$ for 2η binning, covering C values that occur less than once per computational domain (and thus extends to negative values). Figure adapted from HCD99.

found at maximum concentration $C_{\max} = \mathcal{R}^{3-a_{\min}}$ results in $f(a_{\min}) = 0$ for these sets. This can be seen by setting the product of either $F_v(a)$ or $F_v(C)$ and the normalized domain volume \mathcal{R}^3 equal to unity, after allowing for the fact that the F_v are differential functions of their arguments by multiplying them by a_{\min} or C_{\max} , respectively.

Information about higher (less probable) concentrations than are typically found in a volume DL on a side must come from analyzing a large number of realizations of each sample and determining an “annealed” average, where $f(a_{\min}) < 0$ (e.g., Chhabra & Sreenivasan 1991). The annealed version (dashed curve in Fig. 3), also binned by 2η , is well fitted by the function $f(a) = -12.414 + 89.659/a - 132.01/a^2$, for $a > a_{\min} = 2.0$. We have restricted ourselves to 2η binning for the present to preserve good statistics; smaller binning scales sample a deeper cascade and will generate large C values with higher probability. The three sets of $f(a)$ in Figure 3, as binned over 2, 4, and 8 η illustrate the multifractal or “singular” nature of the distribution. For any given Re , smaller a values correspond to larger C values (eq. [9]), and larger values of $f(a)$ imply larger F_v . The smaller a_{\min} , or larger $f(a)$ for $a > a_{\min}$ seen for the smaller binning scales implies that, averaged over a bin, smaller binning scales retain large C far more commonly than larger binning scales. That is, as the scale is reduced, no asymptotic or well-defined limiting local value is reached. Also shown in Figure 3 is the singularity spectrum for dissipation of turbulent kinetic energy (open symbols), which is scale-independent. The agreement between this spectrum and that for particle density binned at the 2η scale is intriguing. The deviation between our spectra (solid symbols and dashed line) and that for dissipation seen toward the right hand side (large a) is due to incomplete sampling of very low particle density regions in

our particle density simulations because of memory limitations on the number of particles we can follow. Dissipation, being a continuously varying function, is not subject to this effect. For this reason, $F_v(>C)$ was less well defined than $F_p(>C)$, which, by definition as a particle rather than volume fraction, is always fully characterized. In any case, our primary interest is in the zones of high concentration (small α).

As a check on the method (subtle normalization issues are discussed in Chhabra et al. 1989), an average $f(a)$, obtained from our calculations at all three Re values was used to calculate $F_p(>C)$ at each of our three Re values, for comparison with the $F_p(>C)$ distributions determined directly from numerical results (HCD99). As shown in Figure 4, the single $f(a)$ does quite well at predicting $F_p(>C)$ at all three Re, even though they all subtended slightly different numbers of integral scales. For any C , $F_p(>C)$ increases with Re and thus \mathcal{R} . This may be puzzling after only a quick inspection of equation (10), since $f(a) - 3$ is always negative (Fig. 3). However, for a fixed C , $a(C)$ increases with \mathcal{R} (eq. [9]), and thus $f(a)$ also increases (Fig. 3), so the exponent in equation (10) becomes less negative. Since any function is more sensitive to its exponent (here $f(a) - 3$) than to its base (here \mathcal{R}), eq. [10] implies $F_p(>C)$ and thus $F_p(>C)$ increase with \mathcal{R} .

5.1.2. Particle Time Histories

The particle time histories are of interest in their own right and illustrate how particles experience a fluctuating background concentration as they wander through the fluid. Figure 5 illustrates histories for several randomly chosen particles. The particles are moving at roughly con-

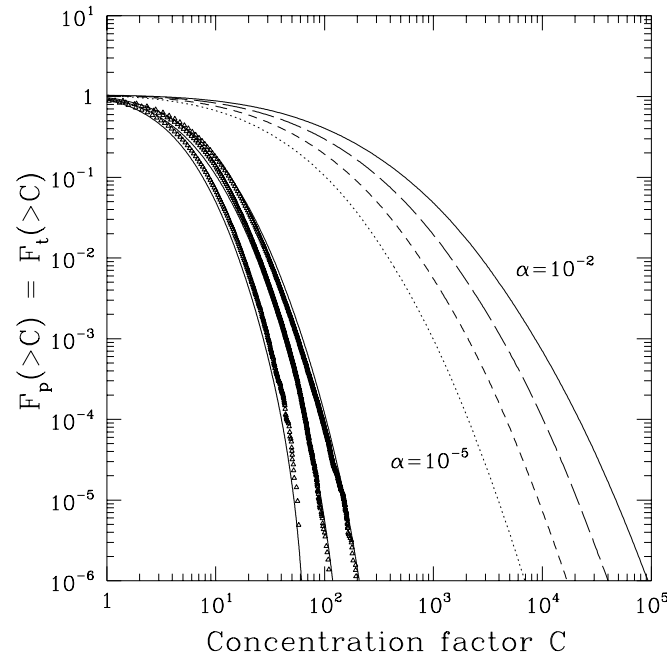


FIG. 4.—Probability distribution functions (PDF's) for the fraction of particles lying in regions with concentration factor greater than C [$F_p(>C)$], or, equivalently, the fraction of time spent by any particle in such regions [$F_t(>C)$]. The three sets of points are binned directly from our numerical simulations; the associated curves are calculated from a single averaged $f(a)$ obtained from all three values of Re (dashed curve in Fig. 3). As discussed in § 5.2, the curves without points use the same $f(a)$ to predict PDF's at the larger Re corresponding to four plausible nebula α values: 10^{-2} (solid line), 10^{-3} (long-dashed line), 10^{-4} (short dashed line), and 10^{-5} (dotted line).

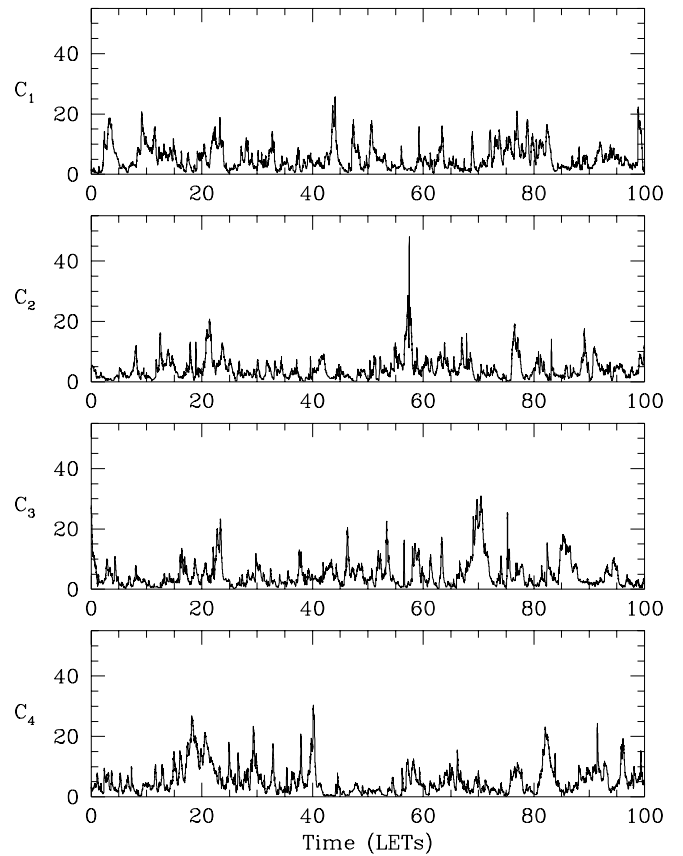


FIG. 5.—Ambient concentration encountered by four different particles moving in three-dimensional turbulence, as a function of time (measured in large eddy turnover times $LET = \omega(L)^{-1}$), without feedback onto the gas. These may also be regarded as a longer history for a single particle. Note how denser regions are encountered less frequently.

stant space velocity (approximately the velocity V_L of the largest eddies, since they are trapped to nearly all eddies), and repeatedly encounter zones of different density with little noticeable effect on their velocity (their stopping time is much longer than the clump transit time η/V_L). In these simulations, where no particle interactions are computed, the particles pass through the dense zones and continue their evolution. The dense zones per se persist for times much longer than the passage time of a single particle (CDH96; She, Jackson, & Orzag 1990). The more numerous, lower density zones are encountered more frequently, and the rare, very high density zones less frequently. This time history, essentially a (convoluted) one-dimensional path through the computational volume, has the same “intermittent” or spiky structure as seen for dissipation (see, e.g., Meneveau & Sreenivasan 1987; Chhabra et al. 1989).

From simulations such as these, we have validated the ergodic assumption that the fraction $F_p(>C)$ (spatially averaged over all particles at several snapshots in time) is equal to the fraction of time $F_t(>C)$ spent by a given particle in regions denser than C (temporally averaged over extended trajectories for a few particles). The comparison is shown in Figure 6. A “random walk” calculation does not accurately reflect this behavior; the particles are not moving randomly through the volume and encountering dense zones with probability given by their volume fraction; rather, particle trajectories are “attracted” to the dense

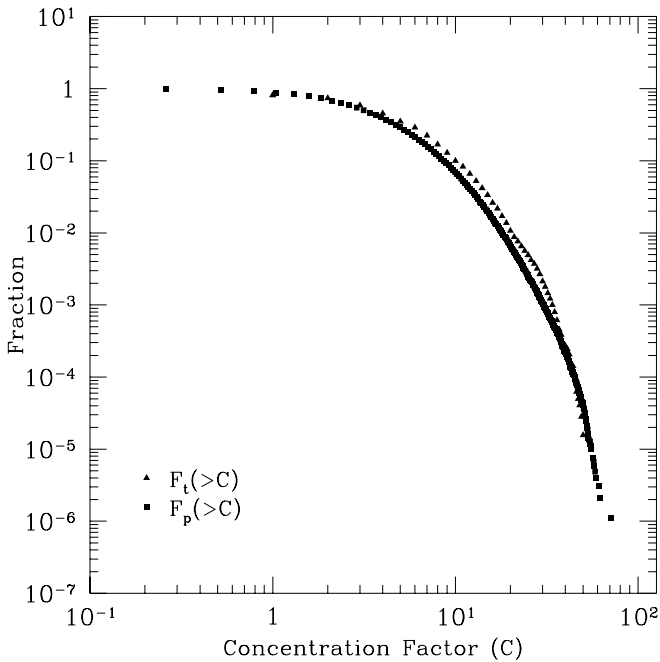


FIG. 6.—Comparison of $F_p(>C)$ from binned data in several snapshots (squares; temporal realizations) containing all particles (as in Fig. 4), with $F_t(>C)$ (triangles), calculated from extended time histories of 16 different particles (as in Fig. 5).

zones, or, probably more physically, repelled from the sparse, complementary eddy zones. This behavior is correctly captured using $F_p(C)$.

5.2. Predictions for Nebula Re

The properties of multifractals make it much easier for us to predict nebula properties than merely making extrapolations from Re values we have studied numerically. In the multifractal context, equation (10), and the Re-independence of $f(a)$, suggest identification of $f(a)$ with the level-independent “rule,” and $\mathcal{R} \propto L/\eta = \text{Re}^{3/4}$ with the number of steps in the cascade. As Re increases, the inertial range (or number of eddy bifurcations) between L and η also increases. The cascade model described by Meneveau & Sreenivasan (1987), mentioned at the beginning of this section, is a specific case of the binomial cascade discussed by Mandelbrot (1989); all provide insight as to how higher C result from a deeper cascade with more steps. Mathematically, equations (9) and (10) show how high C values become more likely.

If $f(a)$ is indeed a Re-independent, universal function for optimally concentrated ($\text{St}_\eta = 1$) particles, we can then predict PDF’s for any Re (i.e., any given nebula α) using equation (10). Several lines of argument support the assumption of a level-independent and Re-independent “rule.” First, our own numerical experiments directly show $f(a)$ to be Re-independent over an order of magnitude in Re (Fig. 3). A second line of argument relates particle concentration to other well-known Re-independent properties. Dissipation of k is physically connected to particle concentration through their mutual preference for the Kolmogorov scale and by the fact that the shapes of the singularity spectra for dissipation, and for particle concentration binned at close to the Kolmogorov scale, are similar (Fig. 3;

HCD99). The singularity spectrum of dissipation has already been connected to the turbulent cascade process (Meneveau & Sreenivasan 1987). Thus, turbulent concentration is probably also closely related to the turbulent cascade process. The turbulent cascade is known to have Re-independent properties in the inertial range. For instance, the $f(a)$ for dissipation has been shown to be Re-independent—from numerical work at $\text{Re} \sim 100$, including our own, through laboratory experiments with $\text{Re} \sim 10^4$, to experimental studies of the atmospheric boundary layer with $\text{Re} \sim 10^6$ (Chhabra et al. 1989; Hosogawa & Yamamoto 1990). Furthermore, it has been directly demonstrated from analysis of observations of dissipation in large Re turbulence that the probability distribution of “partition factors” or “multipliers” is independent of level within the inertial range (Sreenivasan & Stolovitsky 1995). Based on these arguments, we believe and presume that the particle concentration singularity spectrum $f(a)$ remains Re-independent in turbulent cascades with far larger values of Re than those of our numerical experiments. Given this invariance, we can predict nebula conditions more confidently than from extrapolation alone, as was done by CDH96.

We obtain PDF’s at Re which are much larger than directly accessible values by containing the Re-dependence purely within $\mathcal{R} = DL/B\eta = (D/B)\text{Re}^{3/4}$. As argued at the beginning of this section, the $f(a)$ is associated with a certain D and B , which we interpret as being the $D \approx 9$ and $B = 2$ implicit in our $f(a)$ (§ 5.1.1). The nebula \mathcal{R} is then only dependent on Re and easily determined for any turbulent α as $\mathcal{R} = 1/\epsilon = DL/B\eta = (D/B)\text{Re}^{3/4} \approx 4.5\text{Re}^{3/4}$. Recalling $v_m = m_{\text{H}_2} c/2\rho_g \sigma_{\text{H}_2}$ (§ 3),

$$\begin{aligned} \mathcal{R} &= 4.5 \left(\frac{\alpha c H}{v_m} \right)^{3/4} = 4.5 \left(\frac{\alpha \Sigma}{m_{\text{H}_2} / \sigma_{\text{H}_2}} \right)^{3/4} \\ &= 7 \times 10^5 \left(\frac{\Sigma}{430 \text{ g cm}^{-2}} \right)^{3/4} \left(\frac{\alpha}{10^{-4}} \right)^{3/4}. \end{aligned} \quad (11)$$

Also shown in Figure 4 are predictions of $F_p(>C) = F_t(>C)$ for four values of nebula α , using equations (10) and (11). Based on these predictions, $\text{St}_\eta = 1$ particles spend about 1%–10% of their time in regions with $C > 10^3$ under nebula conditions at different α . All curves in Figure 4 assume a minimum mass nebula ($\Sigma = 430 \text{ g cm}^{-2}$ at 2.5 AU), but mass enhancement by some factor \mathcal{F} would play a role similar to α (see also § 3).

6. IMPLICATIONS AND DISCUSSION

6.1. Regions of Moderately High Density

For concentration factors leading to ρ_{ch}/ρ_g at least as large as unity, particle mass loading might start to affect the “partition rules” and change the statistics of the cascade. Nevertheless, several interesting effects can result from concentrations less than this possible limit. If the region in question has an average mass density in solids of $\rho_p = f_{\text{sol}} \rho_g = 5 - 8 \times 10^{-3} \rho_g$ (at, say, 400 K; Pollack et al. 1994), and some fraction $f_{\text{ch}} < 1$ of this amount is in chondrule-sized particles (recalling that other particle sizes are not susceptible to TC), it is clear that C as large as $(f_{\text{sol}} f_{\text{ch}})^{-1}$, at least several hundred (for $f_{\text{ch}} = 1$), remains free of mass loading concerns. If $f_{\text{ch}} \ll 1$, far larger C are allowed. The

point is that, depending on $f_{\text{sol}} f_{\text{ch}}$, C can get quite large without violating the mass loading caveat.

While most of the volume of the nebula is characterized by $C < 100$, Figure 4 shows that chondrules in the nebula spend a significant fraction of their time residing in regions where the particle density is enhanced by a factor of $C > 100$. These results might help us understand why some chondrule types seem to have been heated under unusually oxidizing conditions (e.g., Rubin, Fegely, & Brett 1989), which has been attributed to vaporization of a large ambient density of solids—enhanced by several orders of magnitude over solar—as part of the chondrule formation process (note, however, that it is not universally accepted that the chondrule oxidation state information necessarily implies a large background abundance of oxygen; Grossman 1989).

Several proposed chondrule melting processes—shock waves (Hood & Kring 1996; Connolly & Love 1998) or lightning bolts (Desch & Cuzzi 2000; Desch 2000)—are envisioned to occur ubiquitously within the region of the nebula in which we propose TC operates to sort the chondrules after their formation (for reviews of candidate chondrule melting processes in general see Grossman 1989, Morfill, Spruit, & Levy 1993, Boss 1996, and Jones et al. 2000). Specifically, Desch & Cuzzi (2000) showed that TC itself is an enabling factor in generation of nebula lightning. They found that the optimal conditions for energetic lightning bolts are found in 1000 km regions with $C \sim 100$ —especially if the nebula were denser than “minimum mass” ($\mathcal{F} \sim 10$). Either lightning or shock waves—heating dense zones where the background density of solids is large (see Hood & Horanyi 1993; Hood & Kring 1996; Connolly & Love 1998)—could elevate the local oxygen abundance by evaporating some part of the solids. However, TC does not concentrate “fine dust”—only chondrule-sized particles—so significant local volatilization of some chondrules, or the surfaces thereof, would be implied. Whether this is consistent with mineralogical signatures which are seen in the survivors would be useful to address in the future.

6.2. Encounters with Very Dense Regions

The scenario of CDH96 suggested in a qualitative way that TC could lead to stable, if low-density, clusters or clumps of chondrules as direct precursors of planetesimals. We delineate the logic of this argument, using the PDF's derived in § 5, and then discuss the difficulties with the original scenario.

The PDF's can be combined with the particle velocity through space V_p to calculate the “encounter time” T_{enc} of a chondrule with a region of arbitrary C , using a duty cycle argument. The fraction of time spent by a typical chondrule-size particle in clumps with concentration greater than C , $F_t(>C) \approx t_{\text{in}}(>C)/t_{\text{out}} \approx t_{\text{in}}(>C)/T_{\text{enc}}$, where $t_{\text{in}}(>C) \leq T_{\text{enc}}$ is the time spent traversing a bin with concentration greater than C (§ 5.1.2). Thus, for bins of dimension 2η and particle velocity V_p , $t_{\text{in}}(>C) = 2\eta/V_p$, so $T_{\text{enc}} \approx t_{\text{in}}(>C)/F_t(>C) = t_{\text{in}}(>C)/F_p(>C) = (2\eta/V_p)1/F_p(>C)$, and the encounter rate is $1/T_{\text{enc}} = (V_p/2\eta)F_p(>C)$. We have verified numerically that, as expected for particles with stopping times t_s much shorter than the overturn time of the largest eddies Ω_0^{-1} , V_p is nearly identical to the typical turbulent gas velocity $\sqrt{2k} \approx c\sqrt{\alpha}$ (Völk et al. 1980; Markiewicz, Mizuno, & Völk 1991).

We may calculate the encounter rate (and time) with a cloud so dense that a particle becomes entrapped with its neighbors and possibly removed from further free circulation. Normally, as seen in Figure 5, particles traverse dense regions without incident, because their gas drag stopping time is longer than their transit time (CDH96). An entrapment threshold occurs if interparticle collisions can prevent particles from passing through a cloud; this implies a critical cloud optical depth τ_{coll} of unity, defining a critical C_{coll} . For small, dense 2η -sized clumps, $\tau_{\text{coll}} = 1 = 2\eta C_{\text{coll}}(\bar{\rho}_{\text{ch}}/m)\pi(2r)^2$, where $\bar{\rho}_{\text{ch}} = f_{\text{sol}} f_{\text{ch}} \rho_g$ is the average (unconcentrated) chondrule mass density, $f_{\text{sol}} \approx 5 \times 10^{-3}$ at 400 K is the fractional mass in solids, f_{ch} is the fraction of solids in chondrules, and m and r are chondrule mass and radius. Then

$$C_{\text{coll}} \approx 33r\rho_s/\eta\rho_g f_{\text{ch}} \approx \frac{4 \times 10^5}{f_{\text{ch}}} \left(\frac{10^{-4}\mathcal{F}}{\alpha} \right)^{1/4}. \quad (12)$$

In the final expression above, we have substituted the first expression of equation (8) for the product $r\rho_s$, since the value of this product for optimally concentrated particles is constrained by nebula conditions (§ 3). We substituted the general expression for $\eta = L\text{Re}^{3/4} = (H/\alpha)^{1/4}(v_m/c)^{3/4}$ (~ 0.5 km $(10^{-4}/\alpha)^{1/4}$), and assumed other nominal parameters at 2.5 AU ($\Sigma = 430$ g cm $^{-2}$, $c = 1.5 \times 10^5$ cm s $^{-1}$).

For nominal, minimum mass nebula parameters, assuming $f_{\text{ch}} \approx 1$, and using the PDF's we have in hand (binned at 2η scales), we find that T_{enc} varies between 10^3 years for $\alpha = 10^{-2}$ to 10^8 years for $\alpha = 10^{-4}$. The encounter times are sensitive to nebula parameters adopted and would decrease for smaller binning (e.g., by $B = 1$), or enhanced nebula densities ($\mathcal{F} > 1$). This quantifies the length of time chondrules spend freely wandering before encountering a region in which they are certain to undergo collisions. We suggested earlier that such an encounter at $T_{\text{enc}}(C_{\text{coll}})$ removes the chondrule from further circulation by entrapping it with others in the dense cluster. Alternately, such dense zones might merely provide a large increase in the collisional aggregation rate of optimally sized particles. In fact, if chondrules or groups of chondrules undergo collisional aggregation at low relative velocities (and particles of chondrule size always have low relative velocities in turbulence [Weidenschilling & Cuzzi 1993; Markiewicz et al. 1991]), they may form fractal aggregates with mass proportional to radius squared (Weidenschilling & Cuzzi 1993; Beckwith et al. 2000). The average density of such aggregates is inversely proportional to their bounding “radius,” so they retain the same stopping time as their individual components (individual chondrules), and can continue to participate in TC.

However, before this line of thought can be pursued much further, mass loading (discussed in the next section) must be assessed. Depending on their linear extent, the optically thick clouds described above can reach a mass density orders of magnitude larger than that of the gas, which would probably invalidate our assumption of no feedback. In general, for a clump of mass density ρ_{ch} composed of chondrules of radius r and density ρ_s ,

$$\rho_{\text{ch}} = \frac{r\rho_s\tau_{\text{coll}}}{3B\eta}, \quad \text{or} \quad \frac{\rho_{\text{ch}}}{\rho_g} = \frac{r\rho_s}{3B\eta\rho_g} \text{ for } \tau_{\text{coll}} = 1. \quad (13)$$

In deriving equation (13) we have expressed the linear size of a cluster as $B\eta$. For $\eta \sim 0.5$ km $(10^{-4}/\alpha)^{1/4}$ and $\rho_g = 1.1$

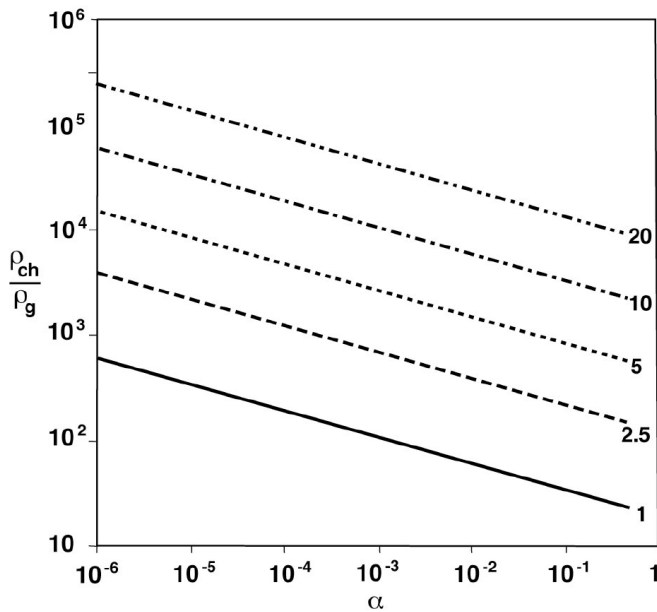


FIG. 7.—Variation of ρ_{ch}/ρ_g with α (for cluster optical depth unity) for the same nebula regions as shown in Fig. 1. The power-law results are labeled by the appropriate distance from the Sun in AU. Regions with more severe turbulence (larger α) select smaller particles for concentration which, having larger area per unit mass, can be concentrated to $\tau_{coll} = 1$ without reaching such large mass loading ratios as under more “nominal” conditions as shown in Fig. 1.

$\times 10^{-10} \text{ g cm}^{-3}$, the particle density exceeds $10\rho_g$ for $\tau_{coll} = 1$ clusters smaller than $(60\text{--}600/\mathcal{F}) \text{ km}$ —about $(100\text{--}1000/\mathcal{F})\eta$ for $r\rho_s$ in the normal range for chondrules $\approx 0.02\text{--}0.2$ (Fig. 1).

6.3. Limitations due to High Mass Loading:

The cascade process model is only valid as long as no new physics emerges at some step in the cascade to change the partition factors, as represented globally by $f(a)$, applicable to subsequent steps in the cascade. However, application of the expressions above for optically thick clusters of scale 2η implies $\rho_{ch}/\rho_g \sim 3000$. While these high concentrations literally relate to regions comparable to η in size, where there is no turbulence to damp, the cascade that is needed to produce such a cluster must have extended to larger sizes in the surrounding “penumbra” where the particle density, while lower, might still be large enough to damp turbulent motions. We have made some preliminary calculations of $f(a)$ from low-Re numerical simulations having average mass loading (defined as the ratio of particle mass density to gas mass density) on the order of unity. Even here, turbulent concentration persists (to local regions with particle mass density more than 30 times the gas mass density), but the $f(a)$ is altered in the sense that high C values have a lower probability. For comparison, unloaded simulations at this Re result in $C_{max} \approx 60$. The magnitude of the mass loading effect is approximately equal and opposite to that of decreasing the bin size from 2η to η . Clearly, this effect must be better quantified before more specific predictions of T_{enc} and chondrule accumulation timescales can be made. Even for small $\alpha \sim 10^{-3}$, the mass loading regime of questionable validity is not a large one (note that eq. [13]) above showed that regions of size 300η , or $100\text{--}300 \text{ km}$, are

probably within the range of validity); however, it is certainly an interesting one. If we combine equations (7) or (8) and (13), we obtain

$$\frac{\rho_{ch}}{\rho_g} = \left(\frac{m_{H_2}}{4\sqrt{2}\sigma_{H_2}} \right)^{1/2} \left(\frac{1}{3\sqrt{2}B\eta} \right) \left(\frac{H}{\alpha\rho_g} \right)^{1/2}, \quad (14)$$

which shows that regions which are denser and/or have more intense turbulence (higher α), such as may have characterized the very early evolutionary stages of the nebula, are less prone to mass loading difficulties. That is, they provide $\tau_{coll} = 1$ at lower ρ_{ch}/ρ_g . Figure 7 shows that conditions at 1AU (gas density $\rho_g \sim 10^{-9} \text{ g cm}^{-3}$), with $\alpha \sim 10^{-2}$ to 10^{-1} , provide $\tau_{coll} = 1$ with $\rho_{ch}/\rho_g < 100$. Full treatment of a wider parameter space, allowance for mass loading and other binning scales B , and connection to hypotheses for chondrule formation (Desch & Cuzzi 2000) and dust rimming (Cuzzi et al. 1999; Morfill & Durisen 1998) that are tied to TC, will be treated in subsequent publications.

7. DISCUSSION

Turbulent concentration promises to provide another tool for our planetesimal construction toolkit. Nominal nebula conditions, including weak turbulence, lead to concentration factors large enough to concentrate chondrule-sized particles to densities greatly exceeding the nominal nebula average. The presence of such dense regions might help us understand some aspects of chondrule formation. Generalization of the physics shows that fluffy aggregates would also be subject to turbulent concentration, but in nebula regions where the gas density is lower and/or the turbulent intensity higher than expected for the terrestrial planet region. If TC is a key aspect of the primary accretion of planetesimals, any chondrules formed or transported to low-density, outer solar system regimes might only have escaped incorporation into planetesimals to a greater degree than in the terrestrial planet region. The size distributions produced by turbulent concentration are in very good agreement with those found in primitive chondrites; however, the fact that most primitive meteorites contain ample evidence for abrasion, fragmentation, and other mechanical processes, which may well have continued long after the nebula gas vanished and aerodynamic processes became irrelevant, warns us that we should not expect any single process to explain all properties of even “primitive” meteorites.

The spatial distributions of concentrated chondrules under nebula conditions can be predicted using the multifractal properties of turbulent concentration. Because of the Re-independent properties of the process, these predictions are far stronger than mere extrapolations to high Re. Various timescales of interest can then be estimated, including the timescale in which a chondrule encounters a cluster so dense that it is entrapped. However, preliminary estimates of timescales for simple accumulation by entrapment in unusually dense clusters are comfortably shorter than nebula lifetimes only for higher α values than those which best explain chondrule size-density products.

Mass loading is expected to change the nature of the process at some point in the cascade where the concentrated particle density becomes comparable to, or greater than, that of the gas. Depending on the mass fraction in solid “chondrules,” this might imply concentration factors as

small as 10^2 —or possibly far larger. Mass loading has not yet been quantitatively treated, but it seems it will inevitably increase the encounter timescales by decreasing the abundance of very dense clusters. Perhaps turbulent concentration only augments collisional accumulation for optimally sized particles.

The evolution of dense clusters in the presence of mass loading and the vertical component of solar gravity deserves study (e.g., Wang & Maxey 1993). Do clusters retain their identity or disperse? Would they be compacted or dispersed by settling, by collisions with other dense clusters en route to, or within the midplane, or by shock waves in the nebula? Perhaps only clusters formed near the midplane avoid the dispersion due to settling.

This research was jointly supported by NASA's Planet-

ary Geology and Geophysics Program and Origins of Solar Systems Program. We thank John Eaton, Kyle Squires, Pat Cassen, Steve Desch, Peter Goldreich, and K. R. Sreenivasan for helpful conversations. We also thank numerous meteoriticist colleagues for their interest and their patient tutorials—especially Ted Bunch, William Skinner, John Wasson, Harold Connolly, Alan Rubin, and Dotty Woolum. The extensive computations on which much of this research is based were made possible by the capabilities of the National Aerospace Simulator (NAS) Program at Ames Research Center; we thank Eugene Tu for extra discretionary time, and Bob Bergeron of the NAS office for computational advice and assistance. We thank the Antarctic Meteorite Working Group for making samples of ALH 85033 and other meteorites available. This research has made use of NASA's Astrophysics Data System Abstract Service.

REFERENCES

- Balbus, S. A., & Hawley, J. F. 1991, *ApJ*, 376, 214
 ———. 1998, *Rev. Mod. Phys.*, 70, 1
 Balbus, S. A., Hawley, J. F., & Stone, J. M. 1996, *ApJ*, 467, 76
 Barge, P., & Sommeria, J. 1995, *A&A*, 295, L1
 Beckwith, S. V. W., & Sargent, A. I. 1991, *ApJ*, 381, 250
 Bell, K. R., Cassen, P., Klahr, H., & Henning, Th. 1997, *ApJ*, 486, 372
 Boss, A. 1996, in *Chondrules and the Protoplanetary Disk*, ed. R. H. Hewins, R. H. Jones, & E. R. D. Scott (Cambridge: Cambridge Univ. Press), 257
 Bracco, A., Chavanis, P. H., Provenzale, A., & Spiegel, E. A. 1999, *Phys. Fluids*, 11, 2280
 Brearley, A. J., & Jones, R. H. 1999, in *Reviews in Mineralogy*, Vol. 36, *Planetary Materials*, ed. J. J. Papike (Washington, DC: Mineralogical Society of America), chap. 3
 Cabot, W., Canuto, V., & Pollack, J. B. 1987, *Icarus*, 69, 387
 Cameron, A. G. W. 1978, *Moon Planets*, 18, 5
 Chhabra, A. B., Meneveau, C., Jensen, V. R., & Sreenivasan, K. R. 1989, *Phys. Rev. A*, 40, 5284
 Chhabra, A. B., & Sreenivasan, K. 1991, *Phys. Rev. A*, 43, 1114
 Chokshi, A., Tielsch, A. G. G. M., & Hollenbach, D. 1993, *ApJ*, 407, 806
 Connolly, H. C., & Love, S. 1998, *Science*, 280, 62
 Cuzzi, J. N., Dobrovolskis, A. R., & Champney, J. M. 1993, *Icarus*, 106, 102
 Cuzzi, J. N., Dobrovolskis, A. R., & Hogan, R. C. 1996, in *Chondrules and the Protoplanetary Disk*, ed. R. H. Hewins, R. H. Jones, & E. R. D. Scott (Cambridge: Cambridge Univ. Press), 35 (CDH96)
 Cuzzi, J. N., et al. 1998, *Lunar and Planetary Science Conf. 29*, CD-ROM, abstract 1443 (Houston: LPI)
 Cuzzi, J. N., Hogan, R. C., & Paque, J. M. 1999, *Lunar and Planetary Science Conf. 30*, CD-ROM, abstract 1271 (Houston: LPI)
 Desch, S. J. 2000, *ApJ*, submitted
 Desch, S. J., & Cuzzi, J. N. 2000, *Icarus*, 143, 87
 Dodd, R. T. 1976, *Earth Planet. Sci. Lett.*, 30, 281
 Dominik, C., & Tielens, A. G. G. M. 1997, *ApJ*, 480, 647
 Dubrulle, B. 1993, *Icarus*, 106, 59
 Dubrulle, B., Sterzik, M., & Morfill, G. E. 1995, *Icarus*, 114, 237
 Eaton, J. K., & Fessler, J. R. 1994, *Int. J. Multiphase Flow* 20, Suppl., 169
 Eisenhour, D. 1996, *Meteoritics*, 31, 243
 Fessler, J. R., Kulick, J. D., & Eaton, J. K. 1994, *Phys. Fluids*, 6, 3742
 Frisch, U., & Parisi, G. 1985, in *Turbulence and Predictability in Geophysical Fluid Dynamics and Climate dynamics*, ed. M. Ghil (Amsterdam: N. Holland)
 Gammie, C. 1996, *ApJ*, 457, 355
 Goldman, I., & Wandel, A. 1994, *ApJ*, 443, 187
 Grossman, J. 1989, in *Meteorites and the Early Solar System*, ed. J. Kerridge, (Tucson: Univ. Arizona Press), 680
 Grossman, J., Rubin, A. E., Nagahara, H., & King, E. A. 1989, in *Meteorites and the Early Solar System*, ed. J. Kerridge, (Tucson: Univ. Arizona Press), 619
 Halsey, T. C., Jensen, M. H., Kadanoff, L. P., Procaccia, I., & Shraiman, B. I. 1986, *Phys. Rev. A*, 33, 1141
 Hartmann, L., Calvet, N., Gullbring, E., & D'Alessio, P. 1998, *ApJ*, 495, 385
 Hayashi, C. 1981, *Prog. Theor. Phys. Suppl.*, 70, 35
 Hewins, R. 1997, *Annu. Rev. Earth Planet. Sci.*, 61
 Hewins, R., Jones, R. H., & Scott, E. R. D. 1996, *Chondrules and the Protoplanetary Disk* (Cambridge: Cambridge Univ. Press)
 Hinze, J. O. 1975, *Turbulence* (2d ed., New York: McGraw-Hill), chap. 3
 Hogan, R. C., & Cuzzi, J. N. 2000, submitted
 Hogan, R. C., Cuzzi, J. N., & Dobrovolskis, A. R. 1999, *Phys. Rev. E*, 60, 1674 (HCD99)
 Hood, L., & Horanyi, M. 1993, *Icarus*, 106, 179
 Hood, L., & Kring, D. 1996, in *Chondrules and the Protoplanetary Disk*, ed. R. H. Hewins, R. H. Jones, & E. R. D. Scott (Cambridge: Cambridge Univ. Press), 265
 Hosogawa, I., & Yamamoto, K. 1990, *Phys. Fluids A*, 2, 889
 Hughes, D. W. 1978, *Earth Planet. Sci. Lett.*, 38, 391
 Jones, R. H., T. Lee, H. C. Connolly, S., Jr., Love, G., & Shang, H. 2000, in *Protostars and Planets IV*, ed. V. Mannings, A. Boss, & S. Russell (Tucson: Univ. Arizona Press), in press
 Kato, S., & Yoshizawa, A. 1997, *PASJ*, 49, 213
 Kennard, E. H. 1938, *Kinetic Theory of Gases* (New York: McGraw-Hill)
 Keubler, K., H. McSween, W. D. Carlson, & Hirsch, D. 1999, *Icarus*, 141, 96
 Klahr, H. 2000a, in *Proc. Two Decades of Numerical Astrophysics*, in press
 ———. 2000b, in *Proc. Disks, Planetesimals, and Planets Tenerife*
 Klahr, H., & Henning, Th. 1997, *Icarus*, 128, 213
 Lin, D. N. C., & Papaloizou, J. 1985, in *Protostars and Planets II*, ed. D. C. Black & M. S. Matthews (Tucson: Univ. Arizona Press), 981
 Lust, R. 1952, *Z. Naturforsch.* 7a, 87
 Lynden-Bell, D., & Pringle, J. E. 1974, *MNRAS*, 168, 603
 MacPherson, G. J., Davis, A. M., & Zinner, E. K. 1995, *Meteoritics*, 24, 297
 MacPherson, G. J., Wark, D. A., & Armstrong, J. T. 1989, in *Meteorites and the Early Solar System*, ed. J. Kerridge (Tucson: Univ. Arizona Press), 746
 Mandelbrot, B. 1989, *Pure Appl. Geophys.*, 131, 5
 Markievicz, W. J., Mizuno, H., & Völk, H. J. 1991, *A&A*, 242, 286
 Maxey, M. R. 1987, *J. Fluid Mech.*, 174, 441
 Meneveau, C., & Sreenivasan, K. R. 1987, *Phys. Rev. Lett.*, 59, 1424
 ———. 1991, *J. Fluid Mech.*, 224, 429
 Metzler, K., Bischoff, A., & Stöffler, D. 1992, *Geochim. Cosmochim. Acta*, 56, 2873
 Morfill, G. E. 1985, in *Les Houches, Session XLI, Birth and Infancy of Stars*, ed. R. Lucas, A. Omont, & R. Stora (Amsterdam: Elsevier), 693
 Morfill, G. E., & Durisen, R. H. 1998, *Icarus*, 134, 180
 Morfill, G. E., Spruit, H., & Levy, E. 1993, in *Protostars and Planets III*, ed. E. H. Levy & J. I. Lunine (Tucson: Univ. Arizona Press), 939
 Paque, J. M., & Cuzzi, J. N. 1997, *Lunar and Planetary Science Conf. 28*, CD-ROM, abstract 1189 (Houston: LPI)
 Pollack, J. B., Hollenbach, D., Beckwith, S., Simonelli, D., Roush, T., & Fong, W. 1994, *ApJ*, 421, 615
 Prinn, R. J. 1990, *ApJ*, 348, 725
 Richard, D., & Zahn, J.-P. 1999, *A&A*, 347, 734
 Rubin, A. E., Fegley, B. C., & Brett, R. 1989, in *Meteorites and the Early Solar System*, ED. J. Kerridge & M. S. Matthews (Tucson: Univ. Arizona Press), 488
 Rubin, A., & Grossman, J. 1987, *Meteoritics*, 22, 237
 Shakura, N. I., & Sunyaev, R. A. 1973, *A&A*, 24, 337
 She, Z.-S., Jackson, E., & Orszag, S. A. 1990, *Nature*, 344, 226
 Skinner, W. R., & Leenhouts, J. M. 1991, *Lunar and Planetary Science Conf. 24*, abstract 1315 (Houston: LPI)
 Squires, K., & Eaton, J. K. 1990, *Phys. Fluids A*, 2, 1191
 ———. 1991, *Phys. Fluids A*, 3, 1169
 Sreenivasan, K. R., & Stolovitsky, G. 1995, *J. Stat. Phys.*, 78, 311
 Stone, J. M., & Balbus, S. A. 1996, *ApJ*, 464, 364
 Suplever, K., & Lin, D. N. C. 2000, *Icarus*, 146, 525
 Tanga, P., Babiano, A., Dubrulle, B., & Provenzale, A. 1996, *Icarus*, 121, 158
 Tennekes, H., & Lumley, J. L. 1972, *A First Course in Turbulence* (Cambridge: MIT Press)
 Völk, H. J., Jones, F. C., Morfill, G. E., & Röser, S. 1980, *A&A*, 85, 316

Wang, L., & Maxey, M. R. 1993, *J. Fluid. Mech.*, 256, 27

Wasson, J. A. 1996, in *Chondrules and the Protoplanetary Disk*, ed. R. H. Hewins, R. H. Jones, & E. R. D. Scott (Cambridge: Cambridge University Press), 45

Weidenschilling, S. J. 1977, *Mon. Notes R. Astron. Soc.*, 180, 57

Weidenschilling, S. J. & Cuzzi, J. N. 1993, in *Protostars and Planets III*, ed. E. Levy & J. Lunine (Tucson: Univ. Arizona Press), 1031

Wood, J. A. 1998, *ApJ*, 503, L101